

# Missing Data Imputation with Adversarially-trained Graph Convolutional Networks

Indro Spinelli<sup>a</sup>, Simone Scardapane<sup>a,\*</sup>, Aurelio Uncini<sup>a</sup>

<sup>a</sup>*Department of Information Engineering, Electronics and Telecommunications (DIET),  
Sapienza University of Rome, Via Eudossiana 18, 00184 Rome, Italy*

---

## Abstract

Missing data imputation (MDI) is a fundamental problem in many scientific disciplines. Popular methods for MDI use global statistics computed from the entire data set (e.g., the feature-wise medians), or build predictive models operating independently on every instance. In this paper we propose a more general framework for MDI, leveraging recent work in the field of graph neural networks (GNNs). We formulate the MDI task in terms of a graph denoising autoencoder, where each edge of the graph encodes the similarity between two patterns. A GNN encoder learns to build intermediate representations for each example by interleaving classical projection layers and locally combining information between neighbors, while another decoding GNN learns to reconstruct the full imputed data set from this intermediate embedding. In order to speed-up training and improve the performance, we use a combination of multiple losses, including an adversarial loss implemented with the Wasserstein metric and a gradient penalty. We also explore a few extensions to the basic architecture involving the use of residual connections between

---

\*Corresponding author. Phone: +39 06 44585495, Fax: +39 06 4873300.  
*Email address:* `simone.scardapane@uniroma1.it` (Simone Scardapane)

layers, and of global statistics computed from the data set to improve the accuracy. On a large experimental evaluation, we show that our method robustly outperforms state-of-the-art approaches for MDI, especially for large percentages of missing values.

*Keywords:* Imputation; Graph neural network; Graph data; Convolutional network

---

## 1. Introduction

While machine learning and deep learning have achieved tremendous results over the last years (Goodfellow et al., 2016), with new breakthroughs arising constantly (e.g., in drug discovery (Chen et al., 2018)), the vast majority of supervised learning methods still require data sets with complete information. At the same time, many real-world problems require dealing with incomplete data, such as in the biomedical or insurance sectors (Van Buuren, 2018). For this reason, flexible missing data imputation (MDI) methods are a fundamental component for widespread adoption of machine learning. In particular, there is the need for powerful *multivariate* imputation methods able to work in a variety of data generation regimes (Yoon et al., 2018).

It has been recognized for a while that data imputation can be framed under a predictive framework, and classical machine learning methods (e.g., for regression and classification) can be adapted for this task (Bertsimas et al., 2017). However, imputation and prediction have some fundamental differences that prevent the straightforward application of prediction algorithms: different inputs in general have different missing components, and the missing data mechanism in practice might not be fully random or in adherence to

the model under consideration (Little and Rubin, 1986). In addition, MDI might be a simple preprocessing step for downstream learning tasks, and in this case performance in terms of reconstruction might not be a perfect proxy for classification/regression accuracy later on.

In general, predictive approaches to MDI can be classified depending on whether they try to build a global model for data imputation, or whether they use similar data points to infer the missing components. Algorithms in the former class include using simple statistics computed from the entire data set (e.g., medians), or more advanced k-NN strategies (Lakshminarayan et al., 1996). In the latter case, instead, we have simple linear models (Lakshminarayan et al., 1996), support vector machines (Wang et al., 2006) or, more recently, deep neural architectures (Yoon et al., 2018). These are surveyed more in-depth in Section 2.1.

We argue that a more powerful technique for MDI should exploit both ideas, i.e., use similar data points for each imputation *and* global models built from the overall data set. In fact, recently a large class of neural network techniques have emerged that are able to model and exploit this kind of structured information (in the form of relationships between examples), by working in the domain of graphs (Bronstein et al., 2017; Battaglia et al., 2018). These models have been applied successfully to a wide range of problems, among which recommender systems (Ying et al., 2018), quantum chemistry (Gilmer et al., 2017), entity extraction from relational data (Schlichtkrull et al., 2018), semi-supervised learning (Kipf and Welling, 2017), and many others. However, to the best of our knowledge these techniques have never been applied to MDI. To overcome this, in this paper we define and carefully

analyze an architecture for MDI based on a specific class of graph neural networks, namely, graph convolutional networks (GCN) (Kipf and Welling, 2017).

### *Contributions of the paper*

Our generic framework for MDI is shown later on in Fig. 1. We frame the overall problem in terms of a GCN autoencoder, that learns to reconstruct the overall data set conditioned on some artificial noise added during the training phase (similar to a classical denoising autoencoder (Vincent et al., 2008)). To build a graph of similarities between points we leverage prior literature on manifold regularization (Belkin et al., 2006), and we describe a simple technique that was found to work well in most situations.

After describing the basic architecture, we also detail three extensions to it that are able to improve either the accuracy or the speed of convergence:

- Firstly, we train the autoencoder with a mixture of standard loss functions and an adversarial loss, which was shown to provide significant improvements for denoising autoencoders in the non-graph case (Yoon et al., 2018).
- Secondly, we motivate another extension with the inclusion of residual connections from the input to the output layer, similar to residual networks (He et al., 2016).
- Finally, we also describe how to include global information on the data set (e.g., means and medians for all feature columns) using a generic context vector in input to the GCN layers.

We test our overall architecture on a large benchmark of data sets with varying levels of noise, showing that it significantly outperform many state-of-the-art approaches, especially for large levels of missing values.

### *Organization of the paper*

The rest of the paper is organized as follows. In Section 2 we describe the relation of this paper with state-of-the-art methods for MDI (Section 2.1) and graph neural networks (Section 2.2). The GCN, which is the building block of our method, is described in Section 3. Then, our graph imputation neural network (GINN) framework and all its extensions are described in Section 4. After a large experimental evaluation in Section 5, we provide some concluding remarks in Section 6.

## **2. Related work**

### *2.1. Missing data imputation*

Algorithms for MDI can be categorized depending on whether they perform univariate or multivariate imputation, and on whether they provide one or multiple imputations for each missing datum (Van Buuren, 2018). In addition, different algorithms can make different theoretical assumptions on whether the data is missing completely at random (MCAR) or not. In this paper we consider multivariate imputation in the MCAR regime, which is standard in the neural network’s literature. In the following we briefly review state-of-the-approaches on this topic, including several algorithms that we will compare to, and discuss their relation with our proposal.

A popular technique for MDI is multiple imputation using chained equations (MICE) (Azur et al., 2011; White et al., 2011; Van Buuren, 2018).

MICE iteratively imputes each variable in the data set by keeping the others fixed, repeating this for multiple cycles, each time drawing one or more observations from some predictive distribution on that variable. Although MICE has shown very good performance in some settings, especially in the bio-medical sector, the assumptions beyond the imputation strategy might result in biased predictions and subsequently lower accuracy.

In the machine learning community, it was recognized very soon that MDI can be framed as a predictive task, on which variants of standard supervised algorithms can be applied, including k-nearest neighbors (k-NN) (Acuna and Rodriguez, 2004), decision trees (Lakshminarayan et al., 1996), support vector techniques (Wang et al., 2006), and several others. However, these techniques have always achieved mixed performance in practice compared to simpler strategies such as mean imputation (Bertsimas et al., 2017). k-NN is limited in making weighted averages of similar feature vectors, while other algorithms are required to build a global model of the data set to be used for imputation. In this paper we also frame the MDI problem in a predictive context, but our proposed model can leverage both global aspects of the data set and local similarities between different points.

More recently, there has been a surge of interest in applying deep learning techniques to the problem of MDI. These include multiple imputation with deep denoising autoencoders (MIDA) (Gondara and Wang, 2018), combinations of deep networks with probabilistic mixture models (Śmieja et al., 2018), recurrent neural networks (Bengio and Gingras, 1996; Che et al., 2018), or generative models including generative adversarial networks (Yoon et al., 2018) and variational autoencoders (Nazabal et al., 2018). Generally speak-

ing, these methods are better at capturing complex correlations in the data (and in the missing data process), thanks to their multiple layers of nonlinear computations, but they still require to build a global model from the data set, ignoring potentially important local contributions from similar points. The method we propose can be seen as an extension both of the MIDA algorithm and of [Yoon et al. \(2018\)](#), but we focus on a more recent class of NNs, graph NNs, to capture local dependencies. We briefly survey the literature on this topic next.

## 2.2. Graph neural networks

Some of the earliest work on extending NNs to the graph domain were presented in [Gori et al. \(2005\)](#); [Scarselli et al. \(2009\)](#), and later reformulated in [Li et al. \(2015\)](#) in a more recent context. These works were mainly motivated by the analogies between unrolled recurrent neural networks and the diffusion of information across a graph.

Another line of work, upon which we build our proposal, considers instead the extension of convolutional neural networks to graph domains under the general term of geometric deep learning ([Defferrard et al., 2016](#); [Kipf and Welling, 2017](#); [Bronstein et al., 2017](#)). This is done by exploiting recent ideas in the field of graph signal processing ([Sandryhaila and Moura, 2013](#); [Sardellitti et al., 2017](#)) to define a more general convolution operator able to work on irregular data structures. In particular, in this work we use the GCN of [Kipf and Welling \(2017\)](#), that for every layer includes a linear diffusion process across neighbors. We note however that many other proposal for graph NNs have been explored recently, which could provide variants of the method we propose here. These include graph attention networks ([Veličković](#)

et al., 2018), non-local NNs (Wang et al., 2018), graph embeddings (Zhang et al., 2018), and graph echo state networks (Gallicchio and Micheli, 2013). An overview of many of these ideas is provided in Battaglia et al. (2018). We explore some of the ideas from Battaglia et al. (2018) in our framework by discussing how to include global information about the data set in the reconstruction process in Section 4.5.

Finally, our work is related to the field of manifold regularization (Belkin et al., 2005, 2006), a semi-supervised class of methods that exploits similarity information among patterns to enforce a regularization term on the optimization process. We build upon them for the construction of our similarity graph, a necessary step for exploiting the power of GNNs.

### 3. Graph convolutional networks

Because the GCN layer is a fundamental building block of our method, we briefly describe it here before moving on to the proposed framework for MDI. Consider a set of  $n$  vertices of a directed graph, whose connectivity is described by a (weighted) adjacency matrix  $\mathbf{A} \in \mathbb{R}^{n \times n}$ , where  $A_{ij}$  is different from 0 if and only if nodes  $i$  and  $j$  are connected. Each node  $i$  has an associated vector of features  $\mathbf{x}_i \in \mathbb{R}^d$ , that we collect row-wise in the matrix  $\mathbf{X} \in \mathbb{R}^{n \times d}$ . We would like to have a generic neural network component able to process simultaneously the features at every node, but also take into consideration their relations, expressed through the adjacency matrix.

One way to extend the idea of convolutional networks to this domain is the so-called graph Fourier transform (Bruna et al., 2013; Sandryhaila and Moura, 2013). Define the Laplacian matrix of the graph as  $\mathbf{L} = \mathbf{D} - \mathbf{A}$ ,



where  $\mathbf{D}$  is the diagonal degree matrix with  $D_{ii} = \sum_{j=1}^n A_{ij}$ . We can perform the eigendecomposition of this matrix as  $\mathbf{L} = \mathbf{U}\mathbf{\Lambda}\mathbf{U}^T$ , where  $\mathbf{U}$  is a matrix collecting column-wise the eigenvectors of  $\mathbf{L}$ , and  $\mathbf{\Lambda}$  is a diagonal matrix with the associated eigenvalues. The equivalent of a classical Fourier transform on a signal can be defined in the graph domain as (Sandryhaila and Moura, 2013):

$$\hat{\mathbf{X}} = \mathbf{U}^T \mathbf{X}, \quad (1)$$

and the inverse transform as  $\mathbf{X} = \mathbf{U}\hat{\mathbf{X}}$ . Using this, a straightforward way to define a convolutional layer on graphs (Bruna et al., 2013) is to first apply the graph Fourier transform, apply a trainable transformation on the frequency components (given by the eigenvalues of the Laplacian), and then back-transform using the inverse Fourier transform. While viable, this approach is however costly and impractical in most cases.

Later authors (Defferrard et al., 2016; Kipf and Welling, 2017) have noted that by applying a restricted class of filters to the frequency components (polynomials), it is possible to work directly in the graph domain using polynomials of the Laplacian itself. In particular, Kipf and Welling (2017) proposed the GCN with the use of linear filters, resulting in the following canonical layer:

$$\mathbf{H}_1 = g(\mathbf{LX}\Theta_1), \quad (2)$$

where  $\Theta_1$  is a matrix of adaptable coefficients, and  $g(\cdot)$  a generic element-

wise activation function, such as the ReLU  $g(s) = \max(0, s)$ .<sup>1</sup> Note that the right-multiplication by  $\Theta_1$  is akin to a classical feedforward layer, while the left-multiplication by  $\mathbf{L}$  allows to propagate the information across the immediate neighbors of each node. Multiple layers of this form can then be stacked to obtain a complete graph NN. Importantly, for a generic network with  $L$  layers, the output of node  $i$  will depend on the outputs of its neighbors up to degree  $L$ .

#### 4. Proposed framework for missing data imputation

We now consider our proposed solution for the MDI problem, which is the main focus of this paper. In MDI, we are also given a data matrix  $\mathbf{X}$ , which has the same size and semantic as in the previous section, but in general no graph information associated with it. Some of the values of  $\mathbf{X}$ , denoted by a binary mask  $\mathbf{M} \in \{0, 1\}^{n \times d}$ , are missing and need to be imputed for downstream processing or classification/regression. We assume to have either numerical features, which are properly normalized, or categorical features that are represented with one-hot encoding. For other types of features, e.g., text, a previous embedding step is needed (Pennington et al., 2014).

Predictive models for MDI described previously in Section 2.1 build a function  $f(\mathbf{x}_i)$  for imputing missing values of a single example  $\mathbf{x}_i$ , but in general, do not exploit directly the potentially important information contained in points that might be similar to it. Here, we propose to model this

---

<sup>1</sup>To avoid some numerical instabilities, it is possible to renormalize the Laplacian to properly bound its eigenvalues, as done in Kipf and Welling (2017). More in general, one can substitute the Laplacian with any valid graph shift operator (Gama et al., 2019).

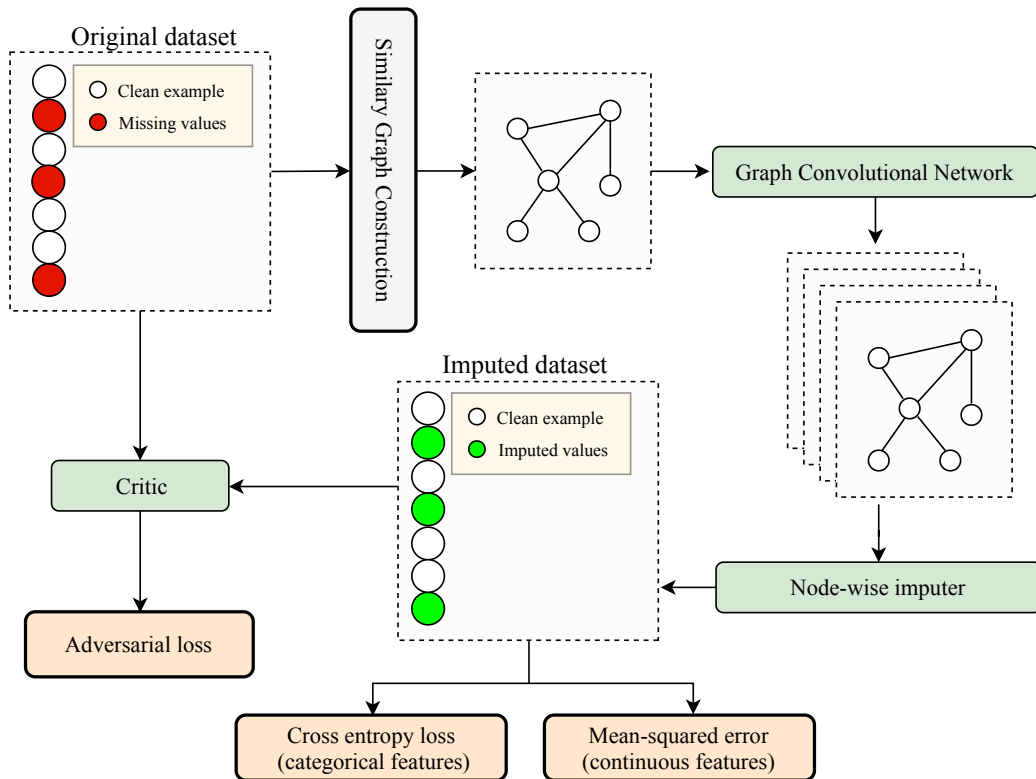


Figure 1: Schematics of the proposed framework for missing data imputation. In green we show the components that are trained end-to-end on the imputation task. In orange we show the different losses. Details on all the steps are provided in the text.

constraint explicitly by building  $f$  using GCN blocks, as shown schematically in Figure 1. To do this, we first need to build a graph of inter-patterns similarities from  $\mathbf{X}$ , as described in the next section.

#### 4.1. Construction of the similarity graph

The first fundamental step of our method is the discovery of the graph structure underneath the tabular representation of the data. In the resulting graph, each feature vector in the data set is encoded as a node of the graph,

while the adjacency matrix  $\mathbf{A}$  is derived from a similarity matrix  $\mathbf{S}$  of the features vectors. As we stated before, constructing a similarity graph from the data is a known problem in the literature, and here we leverage some work from the field of manifold regularization (Belkin et al., 2005, 2006), adapting it for handling the presence of missing data.

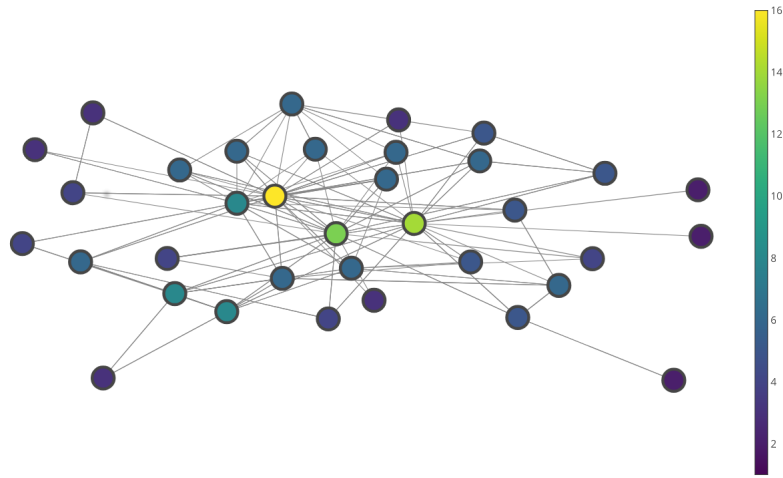
This similarity matrix can be computed using different distance metrics, for the experimental evaluation we opted for the Euclidean distance which was found to work well in practice. This distance is computed pairwise for all features vectors, but each time only the non-zero elements of both vectors are used for the computation:

$$S_{ij} = d(\mathbf{x}_i \odot (\mathbf{M}_i \odot \mathbf{M}_j), \mathbf{x}_j \odot (\mathbf{M}_i \odot \mathbf{M}_j)) \quad (3)$$

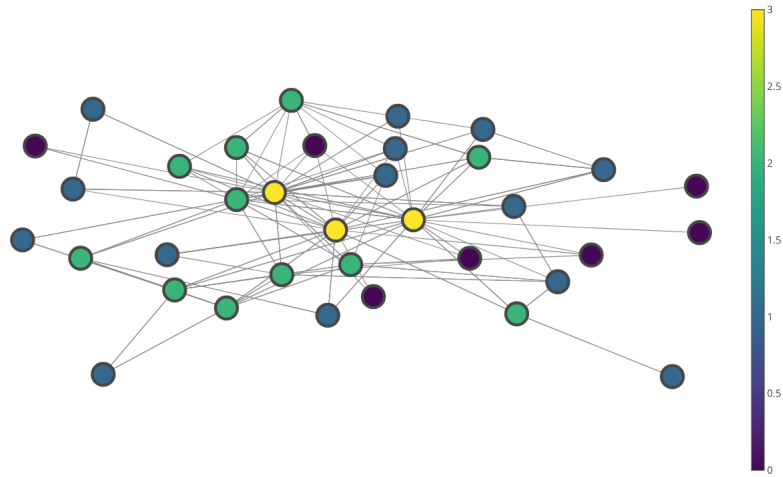
where  $\odot$  stands for the Hadamard product between vectors,  $\mathbf{M}_i$  is the  $i$ th column of the binary matrix  $\mathbf{M}$ , and  $d$  is the Euclidean distance.

In order to have a sparse graph, with meaningful connections between similar nodes, we apply a two-step pruning over the similarity matrix  $\mathbf{S}$ . A first threshold is applied independently over every row of  $\mathbf{S}$ . We compute a percentile for each row that will act as a threshold and only the connections above this threshold inside every row are kept. The second step refines all the selected elements, once again computing a percentile, this time on all the surviving elements of the matrix  $\mathbf{S}$ , and applying another threshold operation. The result is used as adjacency matrix for the GCN in the next section.

We found that the 97.72nd percentile, corresponding to  $+2\sigma$  under a Gaussian assumption, provides good results over all the data sets used in the



(a)



(b)

Figure 2: Subset of the graph reconstructed from the Iris data set using our pipeline. For each node the color intensity represents in (a) the number of connections and in (b) the number of missing features. A clear correlation can be seen between the two.

benchmark of Section 5. Thus, due to the well know 68-95-99 rule, we discard at each step around 95% of all the possible connections. Figure 2 shows a subset of the graph produced with this procedure starting from the Iris data set; here we display the relationship between the number of missing features, 2(a) in a node and its degree 2(b). Interestingly, it can be seen from the figure how nodes with very few non-zero elements will have a higher number of connections, thus it will be easier to reconstruct the values from their neighbors during the imputation process.

#### 4.2. Autoencoder architecture

Autoencoders are composed by an encoder which maps the inputs to an intermediate representation in a different dimensional space  $\mathbf{h} = \text{encode}(\mathbf{x})$ , and a decoder that maps  $\mathbf{h} \in \mathbb{R}^m$  to the original dimensional space  $\hat{\mathbf{x}} = \text{decode}(\mathbf{h})$ . We use  $m > d$  for an overcomplete representation, thus mapping the input into a higher dimensional space with the aim of helping data recovery. Our graph imputer neural network (GINN) will thus be defined as follows:

$$\begin{aligned}\mathbf{H} &= \text{ReLU}(\mathbf{LX}\Theta_1) \\ \hat{\mathbf{X}} &= \text{Sigmoid}(\mathbf{LH}\Theta_2)\end{aligned}\tag{4}$$

where  $\mathbf{L}$  has been defined in Section 3 (the extension to networks with multiple hidden layers being straightforward).

Note that we cannot trivially train the autoencoder on the missing values, because they are not known in the training stage. To solve this, we adopt a denoising version of the autoencoder (Vincent et al., 2008), in which for

every optimization step we add additional masking noise on the input, by the means of an inverted dropout layer applied directly on the input of the network. In particular, at each optimization step, we randomly remove 50% of the remaining inputs. In this way, the autoencoder learns to reconstruct any part of the input matrix, similarly to (Gondara and Wang, 2018).

We train the whole model end-to-end minimizing the reconstruction error over the non-missing elements of the data set. The loss function is thus defined as the combination of a mean squared error (MSE) for the numerical variables and the cross-entropy (CE) for the categorical variables:

$$L_A = \alpha \text{MSE}(\mathbf{X}, \hat{\mathbf{X}}) + (1 - \alpha) \text{CE}(\mathbf{X}, \hat{\mathbf{X}}) \quad (5)$$

where MSE always returns 0 for categorical values and *vice versa* for CE.  $\alpha$  is an additional hyper-parameter that we initialize as the ratio between numerical and categorical columns of the data set. Alternatively, it can be tuned like the other hyper-parameters of the network, although we have not found any definite improvement in doing so.

#### 4.3. Adversarial training of the autoencoder

In order to speed up training, we use an additional adversarial training strategy where a critic, a feedforward network in our case, learns to distinguish between imputed and real data. This is inspired by generative adversarial networks (Goodfellow et al., 2014) and was found to have significant effects in several reconstructions tasks, particularly in the medical domain (Ker et al., 2018).

To train jointly autoencoder and critic and have a stable training we used the Wasserstein distance introduced in Arjovsky et al. (2017), which is infor-

mally defined as the minimum cost of transporting mass in order to transform a distribution  $q$  into a distribution  $p$ . Using the Kantorovich-Rubinstein duality (Villani, 2008) the objective function is obtained as follows:

$$\min_A \max_{C \in \mathcal{D}} \mathbb{E}_{\mathbf{x} \sim \mathbb{P}_{real}} [C(\mathbf{x})] - \mathbb{E}_{\hat{\mathbf{x}} \sim \mathbb{P}_{imp}} [C(\hat{\mathbf{x}})] \quad (6)$$

where  $\mathcal{D}$  is the set of 1-Lipschitz functions,  $\mathbb{P}_{imp}$  is the model distribution implicitly defined by our GCN autoencoder  $\hat{\mathbf{x}} = A(\mathbf{x})$ , and  $\mathbb{P}_{real}$  is the unknown data distribution. Practically, Eq. (6) can be computed by drawing random mini-batches of data and approximating expectations with averages.

The original loss in Arjovsky et al. (2017) used weight clipping to force the Lipschitz property. A further step towards training stability, introduced in Gulrajani et al. (2017), is to use a gradient penalty instead of the weight clipping, obtaining the final loss:

$$L_C = \mathbb{E}_{\hat{\mathbf{x}} \sim \mathbb{P}_{imp}} [C(\hat{\mathbf{x}})] - \mathbb{E}_{\mathbf{x} \sim \mathbb{P}_{real}} [C(\mathbf{x})] + \lambda \mathbb{E}_{\tilde{\mathbf{x}} \sim \mathbb{P}_{\tilde{\mathbf{x}}}} [(\|\nabla_{\tilde{\mathbf{x}}} C(\tilde{\mathbf{x}})\|_2 - 1)^2] \quad (7)$$

where  $\lambda$  is an additional hyper-parameter. We define  $\mathbb{P}_{\tilde{\mathbf{x}}}$  as sampling uniformly from the combination of the real distribution  $\mathbb{P}_{imp}$  and from the distribution resulting from the imputation  $\mathbb{P}_{imp}$ . This means that the feature vector  $\tilde{\mathbf{x}}$  will be composed by both real and imputed elements in almost equal quantity. This distance is continuous and differentiable thus, the more we train the critic, the more reliable the gradients are. Following standard practice in the GAN literature, in our implementation the GCN autoencoder is trained once for every five optimization steps of the critic, and the total loss becomes:



$$L_D = L_A - \mathbb{E}_{\hat{\mathbf{x}} \sim \mathbb{P}_{imp}} [C(\hat{\mathbf{x}})] \quad (8)$$

since it must fool the critic and minimize the reconstruction error at the same time.

#### 4.4. Including skip connections in the model

The autoencoder itself generates an approximate reconstruction of the data set, while the critic loss guides the autoencoder in this process. However, our main scope is the imputation of values not present in the data. For this task we want a greater contribution coming from the most similar nodes. For this reason, we introduce an additional skip layer which consists always in a graph convolution operation but propagating the information across the immediate neighbors of each node without the node itself. This prevents the autoencoder from learning the identity function.

The decoding layer becomes:

$$\hat{\mathbf{X}} = \text{Sigmoid} \left( \mathbf{LH}\boldsymbol{\Theta}_2 + \tilde{\mathbf{L}}\mathbf{X}\boldsymbol{\Theta}_3 \right) \quad (9)$$

where  $\tilde{\mathbf{L}}$  is computed as described in Section 3 starting from an adjacency matrix without self loops. This is shown schematically in Fig. 3.

#### 4.5. Including global statistics from the data set

Another extension we explore is the possibility of including global information on the data set during the computation of the autoencoder. The inclusion of a global set of attributes, in the context of graph neural networks, was described in-depth by Battaglia et al. (2018).

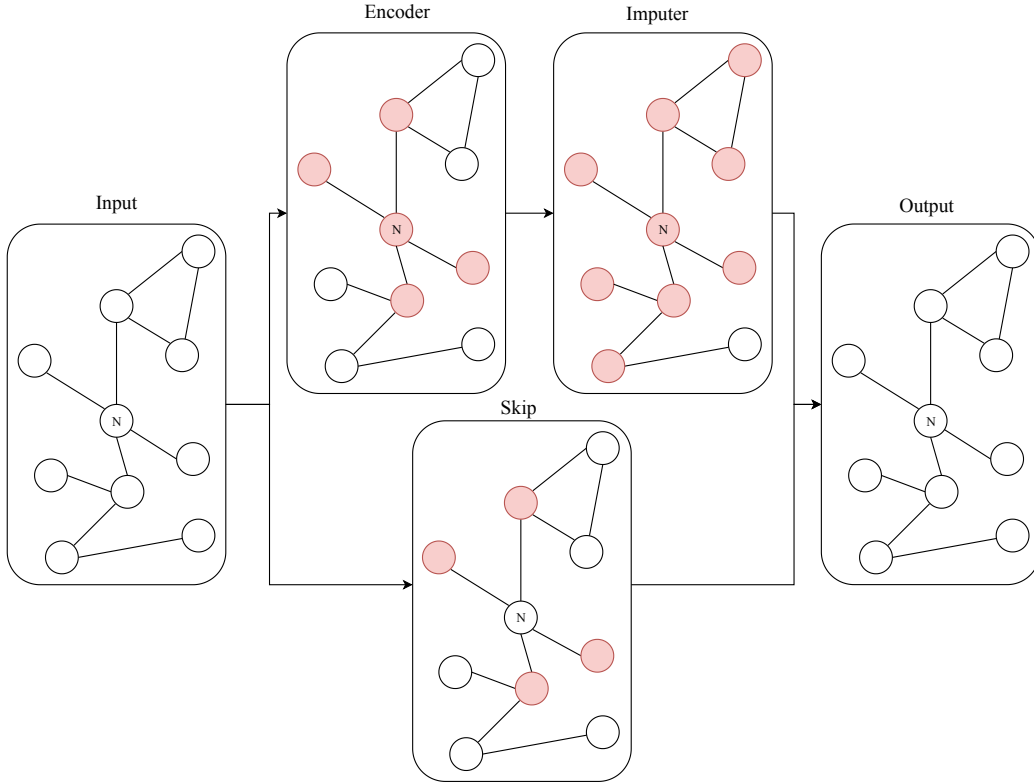


Figure 3: Schematics of the graph autoencoder with the skip connection. We highlight the nodes involved, directly or indirectly by the convolution for the update of the node  $\mathbf{N}$ . The encoding phase involves 1-hop neighbors, decoding/imputation phase instead involves nodes up to 2-hops. The skip connections involves 1-hop neighbors without considering node  $\mathbf{N}$ .

As a proof of concept, in our case we set as global attribute vector  $\mathbf{g}$  for the graph some statistical information of the data set, including mean or mode of every attribute. The global component can be taken into account in the last layer, weighting their contribution for the update of each node:

$$\hat{\mathbf{X}} = \text{Sigmoid} \left( \mathbf{LH}\Theta_2 + \tilde{\mathbf{L}}\mathbf{X}\Theta_3 + \Theta_4\mathbf{g} \right) \quad (10)$$

In addition, if the computation of the global information is differentiable, we can compute a loss term with respect to the global attributes of the original data set:

$$L = L_d + \gamma \text{MSE}(\text{global}(\hat{\mathbf{X}}), \text{global}(\mathbf{X})) \quad (11)$$

where  $\gamma$  is some additional weighting term.

## 5. Experimental evaluation

We used 20 real-world data sets from the UCI Machine Learning Repository (Dua and Graff, 2017) to evaluate the imputation performances, whose characteristics are summarized in Table 1. This selection contains categorical, numerical, and mixed data sets, ranging from 150 observation to 30000 and from only 4 attributes to almost 40. Every data set is divided into training 70% and test 30% sets. Missingness is introduced completely at random on the training set with 4 different levels of noise: 10%, 20%, 30%, and 50%. Our evaluation will focus both on imputation performance as described in Section 5.1 and on the accuracy of post-imputation prediction in Section 5.2. For the benchmark, we used an embedding dimension of the hidden layer of 128, sufficient for an overcomplete representation for all the data sets involved, and trained the model for a maximum of 10000 epochs with an early stopping strategy for the reconstruction loss over the known elements. The critic used is a simple 3-layer feed-forward network trained 5 times for each optimization step of the autoencoder. We used the Adam optimizer Kingma and Ba (2014) for both networks with a learning rate of  $1 \times 10^{-3}$  and  $1 \times 10^{-5}$  respectively for autoencoder and critic.

All the code for replicating our experiments and using the GINN algorithm is released as an open-source library on the web.<sup>2</sup>

### 5.1. Imputation Performance

This evaluation focuses on the comparison of MAE and RMSE between GINN and 6 other state-of-the-art imputation algorithms: MICE (van Buuren and Groothuis-Oudshoorn, 2011), MIDA (Gondara and Wang, 2018), MissForest (Stekhoven and Buehlmann, 2012), mean (Little and Rubin, 1986), matrix factorization and k-NN imputation (Botstein et al., 2001). Concerning MICE and MissForest we used the default parameters. We used  $1 \times 10^{-3}$  and  $1 \times 10^{-4}$  as learning rate for matrix factorization and MIDA with the latter being a 2-layer with 128 units per layer network like our embedding dimension. Finally, we let  $k = 5$  for the k-NN. The imputation accuracy for each data set is presented in Table 2 for the scenario in which 30% of the entries are missing, assuming MCAR, while the results all other levels of missingness are presented in the supplementary material.

To provide a more schematic comparison, in Figure 4 we show the summary of those results for every level of missing data. In these histograms, we provide the number of times that each method achieves the best imputation, i.e. the lowest RMSE in Fig. 4(a) and MAE in Fig. 4(b). Concerning the lower percentage of missing elements (10%, 20%) our method is almost on par with the best among the algorithms tested, i.e., MissForest. When those percentages increase our method brings a huge improvement over the state-of-the-art with the highest difference at 50% where our method significantly

---

<sup>2</sup><https://github.com/spindro/GINN>

Name	observations	numerical attr.	categorical attr.
abalone	4177	8	0
anuran-calls	7195	22	3
balance-scale	625	4	0
breast-cancer-diagnostic	569	30	0
car-evaluation	1728	0	6
default-credit-card	30000	13	10
electrical-grid-stability	10000	14	0
heart	303	8	5
ionosphere	351	34	0
iris	150	5	0
page-blocks	5473	10	0
phishing	1353	0	9
satellite	6435	36	0
tic-tac-toe	958	9	0
turkiye-student-evaluation	5820	0	32
wine-quality-red	1599	11	0
wine-quality-white	4898	11	0
wine	178	13	0
wireless-localization	2000	7	0
yeast	1484	8	0

Table 1: Data sets used for the benchmark. All of them were downloaded from the UCI repository.

outperforms all other techniques. Aggregating the results obtained at 30% and 50% percentage of missing features, we have that our method is the best

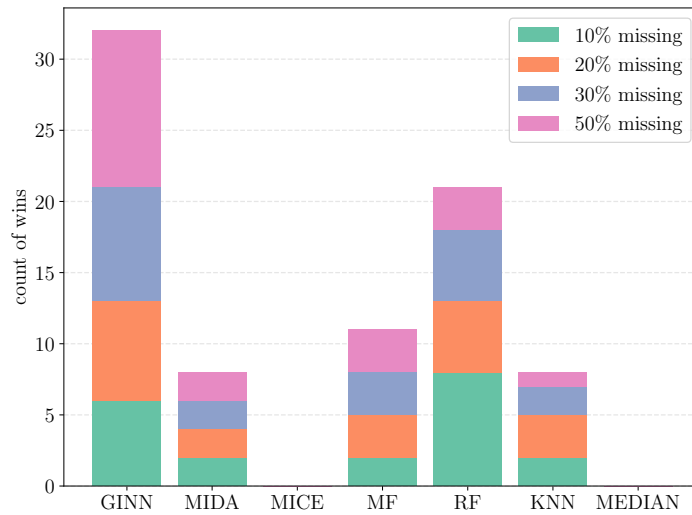
in 50% of the cases against the 27.5% of its best competitor MissForest, when looking at the MAE, and 47.5% against 20% for the RMSE.

MAE	GINN	MIDA	MICE	MF	RF	k-NN	MEDIAN
abalone	0.272	0.390	0.334	1.403	<b>0.224</b>	0.354	0.410
anuran-calls	0.044	0.134	0.050	0.054	0.053	<b>0.033</b>	0.126
balance-scale	0.313	<b>0.234</b>	0.335	0.272	0.308	0.336	0.333
breast-cancer-diagnostic	10.823	24.341	8.315	4.502	<b>2.850</b>	7.341	24.077
car-evaluation	<b>0.395</b>	0.404	0.404	0.714	0.404	0.405	0.421
default-credit-card	3089.320	3387.744	3131.961	2732.639	<b>1521.104</b>	2479.753	4059.687
electrical-grid-stability	0.880	1.069	0.927	<b>0.839</b>	0.853	1.048	0.939
heart	<b>2.854</b>	7.472	3.391	3.034	2.986	3.937	3.146
ionosphere	0.259	0.964	0.312	94.334	0.228	<b>0.216</b>	0.386
iris	0.270	1.399	0.289	<b>0.073</b>	0.262	0.334	0.834
page-blocks	124.401	334.610	629.399	161.999	<b>35.545</b>	119.818	189.061
phishing	<b>0.243</b>	0.401	0.391	0.353	0.368	0.289	0.332
satellite	4.725	8.673	3.406	3.341	<b>2.622</b>	3.230	14.445
tic-tac-toe	<b>0.331</b>	0.442	0.432	0.667	0.450	0.391	0.387
turkiye-student-evaluation	<b>0.081</b>	0.152	0.288	0.082	0.095	0.092	0.265
wine	<b>10.892</b>	33.689	13.032	13.376	12.134	12.493	21.365
wine-quality-red	<b>2.467</b>	3.182	2.964	2.839	2.515	2.761	3.109
wine-quality-white	3.771	5.070	3.861	15.219	<b>3.224</b>	3.922	4.661
wireless-localization	3.632	6.330	3.596	<b>1.045</b>	3.061	3.668	6.302
yeast	<b>0.052</b>	0.111	0.061	0.063	0.052	0.056	0.058

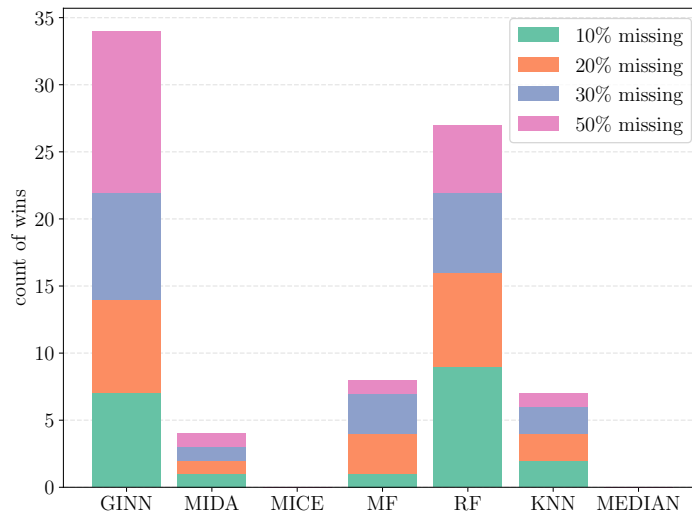
Table 2: Mean Absolute Error with 30% of missing elements.

## 5.2. Predictive Performance

Now we evaluate the performance of standard machine learning algorithms for classification, both binary and multi-class, trained on the various imputations analyzed previously. We consider 4 different classifiers: a k-NN classifier with  $k = 5$ , regularized logistic regression, C-Support Vector Classification with an RBF kernel and a random forest classifier with 10 estimators



(a) Comparison over MAE



(b) Comparison over RMSE

Figure 4: Number of data sets in which each MDI method achieves (a) lowest MAE or (b) lowest RMSE from the true values. The different colors of the bar stand for different percentages of missing elements: from the bottom 10% the lowest to the top 50% the highest.

RMSE	GINN	MIDA	MICE	MF	RF	k-NN	MEDIAN
abalone	0.904	1.190	1.069	3.321	<b>0.811</b>	1.072	1.112
anuran-calls	0.070	0.187	0.076	0.091	0.154	<b>0.058</b>	0.226
balance-scale	0.559	<b>0.436</b>	0.579	0.521	0.516	0.580	0.577
breast-cancer-diagnostic	54.633	114.390	38.122	23.559	<b>21.155</b>	39.653	127.645
car-evaluation	<b>0.623</b>	0.632	0.636	0.845	0.636	0.636	0.649
default-credit-card	17479.409	19664.115	15687.056	15212.927	<b>12897.406</b>	17294.412	23708.027
electrical-grid-stability	1.534	1.857	1.637	<b>1.474</b>	1.536	1.763	1.555
heart	<b>10.883</b>	25.212	12.326	11.367	11.368	14.846	11.708
ionosphere	0.425	1.118	0.462	340.257	0.407	<b>0.380</b>	0.551
iris	0.349	1.792	0.379	<b>0.106</b>	0.333	0.446	1.159
page-blocks	<b>536.645</b>	1035.750	1889.068	795.441	579.227	604.171	869.476
phishing	<b>0.493</b>	0.529	0.625	0.594	0.606	0.548	0.581
satellite	6.256	11.528	4.481	4.562	<b>3.634</b>	4.523	18.335
tic-tac-toe	<b>0.469</b>	0.576	0.657	0.816	0.671	0.625	0.622
turkiye-student-evaluation	0.295	<b>0.285</b>	0.537	0.287	0.292	0.303	0.515
wine	<b>47.901</b>	154.344	52.358	54.764	48.672	54.636	99.651
wine-quality-red	<b>8.099</b>	10.313	9.092	8.883	8.414	9.752	10.265
wine-quality-white	11.188	15.383	11.174	41.324	<b>10.350</b>	12.454	13.432
wireless-localization	4.851	8.470	4.728	<b>1.863</b>	4.214	4.995	8.588
yeast	<b>0.085</b>	0.162	0.090	0.093	0.086	0.091	0.102

Table 3: Root Mean Square Error with 30% of missing elements.

and a maximum depth of 5. All hyper-parameters are initialized with their default values in the scikit-learn implementation.

The classification accuracy is presented in Table 4 for the scenario in which 30% of the entries in the data matrix are missing, assuming MCAR, with a random forest classifier. In Figure 5 we show the summary of the results for each noise level and for each classifier. In these histograms we analyze the number of times each imputation technique allows the classifier to achieve the best accuracy. In this comparison, we consider also the draws.

Our method outperforms competitors with every classification algorithm



tested, and it has the highest number of wins, winning in 85.62% of the cases. Our method worked very well when paired with SVC and Random forest, improving the accuracy for every percentage of missing elements. With the logistic regression and k-NN classifiers, at the lowest missing percentage (10%), our method is slightly below the state-of-the-art. As missing percentages increase, we have a huge improvement over the other competitors. This reflects in the findings of the previous Section and confirms the ability of our method of being very successful in the case of moderate to severely damaged data sets.

### 5.3. Ablation study

To investigate how much every additional step described in Section 4 improves our method, we supervised the quality of imputation and convergence by starting from a basic autoencoder. As the starting point we used a 2-layer denoising autoencoder (DAE), obtained by setting the adjacency matrix to be the identity, obtaining a method similar to (Gondara and Wang, 2018). Then we introduced the graph and the graph convolutional layer in our imputer (GINN) followed by the addition of the critic and the adversarial training (A-GINN), the skip connection (A-GINN skip) and finally the global attributes (A-GINN skip global).

Regarding imputation performances, Table 5 shows how the introduction of the graph and the graph-convolution operation over three randomly selected datasets makes a huge difference against a standard autoencoder. After that, each following step helps to refine even further the imputation accuracy. The reconstruction loss in Eq. (5), more precisely its logarithm, shows a similar behaviour, shown in Fig. 6. After each step we have a better

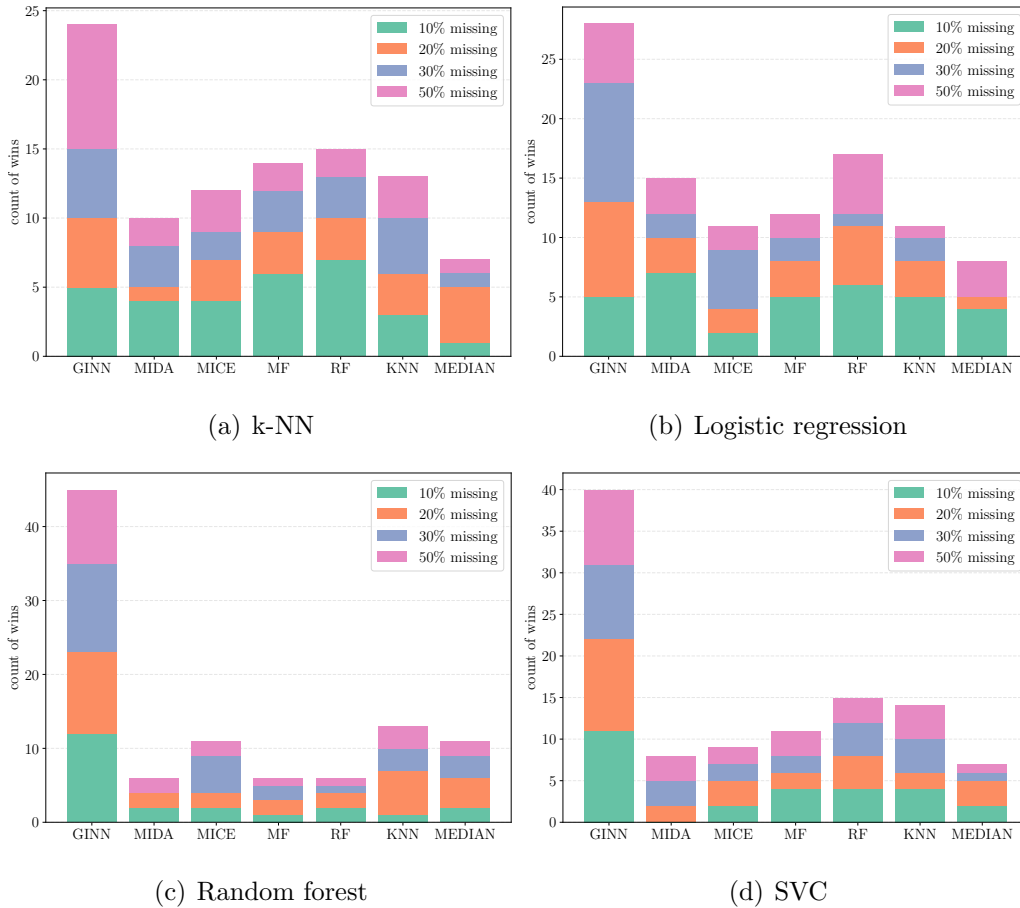


Figure 5: Number of data sets in which each MDI method achieves the highest classification accuracy for each classifier used. The different colors of the bar stand for different percentages of missing elements: from the bottom 10% the lowest to the top 50% the highest.

convergence. Similar results are obtained for all the other datasets.

#### 5.4. Imputation over unseen data

Finally, we test the ability of the model of imputing a new damaged portion of the data set that was not available at training time. In order to

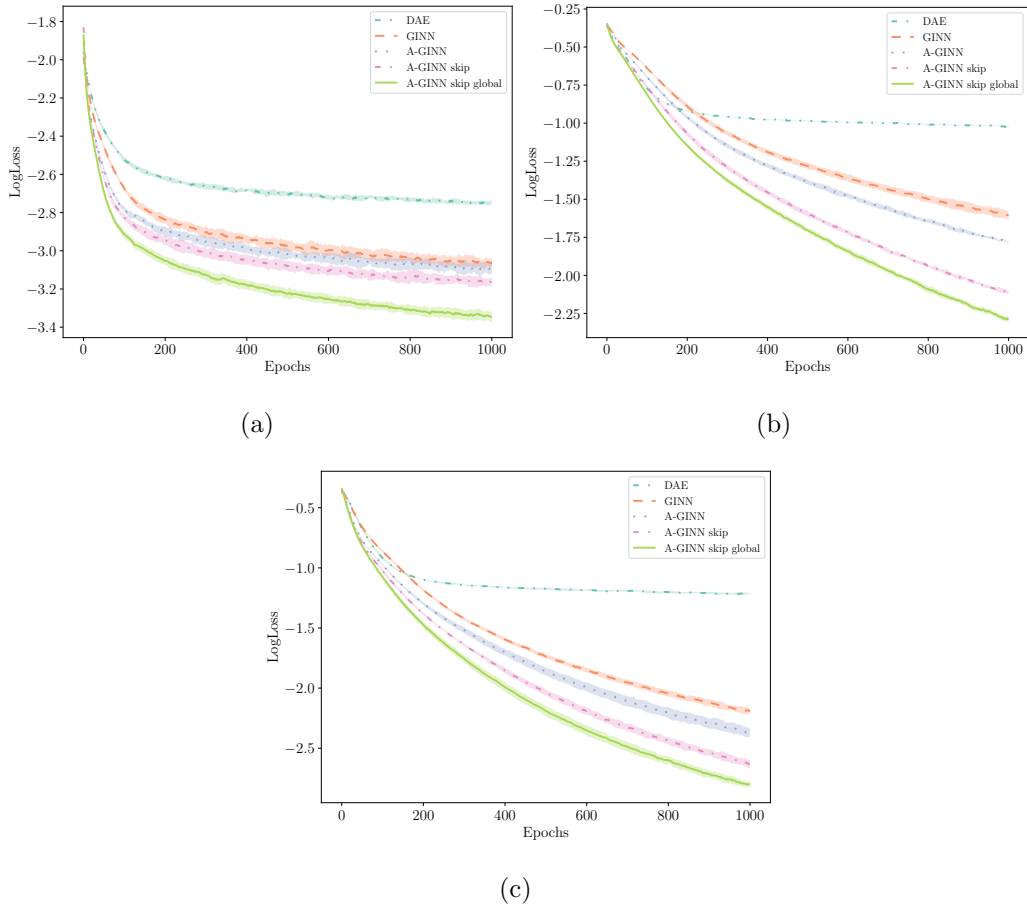


Figure 6: Convergence of the logarithmic loss function defined in Equation 5, on the Ionosphere (a), Tic-Tac-Toe (b) and Phishing (c) data sets for each improvement described in this section and with imputation results shown in Table 5.

Random forest	baseline	GINN	MIDA	MICE	MF	RF	k-NN	MEDIAN
abalone	53.269	<b>55.821</b>	53.269	54.944	51.754	52.472	53.030	51.674
anuran-calls	92.728	<b>94.441</b>	89.810	91.848	93.191	92.635	91.060	90.412
balance-scale	81.328	76.595	72.340	76.595	77.659	76.063	<b>78.723</b>	69.148
breast-cancer-diagnostic	97.076	96.491	95.906	94.736	94.152	97.076	96.491	<b>97.660</b>
car-evaluation	70.520	<b>72.832</b>	71.483	69.942	69.942	70.712	70.520	69.942
default-credit-card	77.870	<b>77.980</b>	77.880	77.880	77.886	77.893	77.9	77.9
electrical-grid-stability	98.533	91.100	86.634	97.556	94.990	97.867	98.700	<b>99.360</b>
heart	82.417	<b>83.516</b>	73.626	<b>83.516</b>	78.021	82.417	82.417	76.923
ionosphere	90.566	<b>95.283</b>	84.905	92.452	92.452	92.452	<b>95.283</b>	93.396
iris	91.111	88.889	80.000	<b>93.334</b>	91.112	91.112	<b>93.334</b>	86.667
page-blocks	94.640	<b>95.066</b>	94.823	94.762	94.640	94.640	94.884	94.701
phishing	84.729	<b>84.482</b>	83.004	83.251	83.990	83.004	84.236	82.019
satellite	83.990	<b>83.850</b>	81.699	82.550	83.650	83.300	83.500	79.950
tic-tac-toe	69.443	72.569	68.056	67.708	67.361	65.972	71.180	<b>72.916</b>
turkiye-student-evaluation	84.020	<b>84.650</b>	84.593	81.214	<b>84.650</b>	83.276	83.505	83.218
wine	96.296	<b>98.148</b>	92.592	<b>98.148</b>	94.444	<b>98.148</b>	94.444	94.444
wine-quality-red	63.334	62.708	62.083	61.667	<b>63.334</b>	62.291	61.458	58.125
wine-quality-white	52.108	<b>53.673</b>	51.360	52.517	52.312	53.265	51.020	51.836
wireless-localization	97.166	96.334	93.167	<b>97.334</b>	96.667	97.000	95.834	97.167
yeast	55.156	56.502	46.188	<b>58.071</b>	43.721	54.484	56.502	53.363

Table 4: Classification accuracy on each data set using a Random forest classifier. The model was trained over the imputed data by algorithms for 30% MCAR. In the first column (baseline) we have the accuracy obtained utilizing the undamaged data set.

impute these new values, we have first to inject the new data in the graph, adding nodes and edges. We compute a new similarity matrix for the new features and also the similarity between these new features and the older ones. Then we add the new nodes to the graph and the edges resulting from the double threshold procedure described in Section 4.1.

To evaluate this, we introduced missing values and evaluated the imputation performances with and without fine tuning the model on a second

	Ionosphere	Tic-Tac-Toe	Phishing
DAE	$0.301 \pm 0.009$	$0.384 \pm 0.001$	$0.314 \pm 0.005$
GINN	$0.263 \pm 0.003$	$0.319 \pm 0.007$	$0.243 \pm 0.017$
A-GINN	$0.260 \pm 0.002$	$0.313 \pm 0.009$	$0.240 \pm 0.016$
A-GINN skip	$0.259 \pm 0.001$	$0.312 \pm 0.005$	$0.239 \pm 0.016$
A-GINN skip global	$0.257 \pm 0.000$	$0.309 \pm 0.001$	$0.238 \pm 0.014$

Table 5: Mean Absolute Error,  $\pm$  the standard deviation, of the imputation over 3 trials with 20% of missing elements. Each data set has the corresponding convergence shown in Figure 6.

randomly kept portion of the data sets. In Table 6 we show the MAE of the imputation over this new portion of data set and compare against the other MDI algorithms. We used the same data set and settings of the ablation study. The fine-tuned version consist of an additional 500 epochs of training over the new graph. It can be seen how our method is able to perform a state-of-the-art imputation on new unseen data without performing additional training and how it improves in case of a small number of additional optimization steps.

## 6. Conclusions and future work

In this paper we introduced a novel technique for missing data imputation, where we used a novel graph convolutional autoencoder to reconstruct the full data set. We also describe several improvement to our technique, including the use of an adversarial loss, and the inclusion of global information from the data set in the reconstruction phase. We showed through

MAE	Ionosphere	Tic-Tac-Toe	Phishing
GINN	<u>0.252</u>	<u>0.320</u>	<u>0.242</u>
GINN (FT)	<b>0.235</b>	<b>0.299</b>	<b>0.237</b>
MIDA	0.782	0.390	0.422
MICE	0.335	0.414	0.644
MF	0.312	0.667	0.462
RF	0.254	0.456	0.344
k-NN	<b>0.235</b>	0.400	0.282
MEDIAN	0.362	0.388	0.343

Table 6: Mean Absolute Error of the imputation with 20% of missing elements.

an extensive numerical simulation that our method significantly outperforms state-of-the-art approaches for missing data imputation, especially for large values of noise, both in terms of reconstruction error and in terms of classification/regression accuracy when the reconstructed data set is used in a downstream supervised learning algorithm.

Future work can consider the adoption of different graph neural architectures for the autoencoding process, or the extension to other types of noisy data beyond vector-valued data. In addition, we can think of training our imputation module together with a classification step in an end-to-end fashion. We leave this to a future work. Finally, we plan on investigating mini-batching strategies on the graph to improve the computational complexity of the method.

## References

## References

- Acuna, E., Rodriguez, C., 2004. The treatment of missing values and its effect on classifier accuracy, in: Classification, clustering, and data mining applications. Springer, pp. 639–647.
- Arjovsky, M., Chintala, S., Bottou, L., 2017. Wasserstein generative adversarial networks, in: Proc. 34th International Conference on Machine Learning (ICML), pp. 214–223.
- Azur, M.J., Stuart, E.A., Frangakis, C., Leaf, P.J., 2011. Multiple imputation by chained equations: what is it and how does it work? International Journal of Methods in Psychiatric Research 20, 40–49.
- Battaglia, P.W., Hamrick, J.B., Bapst, V., Sanchez-Gonzalez, A., Zambaldi, V., Malinowski, M., Tacchetti, A., Raposo, D., Santoro, A., Faulkner, R., et al., 2018. Relational inductive biases, deep learning, and graph networks. arXiv preprint arXiv:1806.01261 .
- Belkin, M., Niyogi, P., Sindhvani, V., 2005. On manifold regularization, in: AISTATS.
- Belkin, M., Niyogi, P., Sindhvani, V., 2006. Manifold regularization: A geometric framework for learning from labeled and unlabeled examples. Journal of Machine Learning Research 7, 2399–2434.

- Bengio, Y., Gingras, F., 1996. Recurrent neural networks for missing or asynchronous data, in: *Advances in Neural Information Processing Systems*, pp. 395–401.
- Bertsimas, D., Pawlowski, C., Zhuo, Y.D., 2017. From predictive methods to missing data imputation: An optimization approach. *Journal of Machine Learning Research* 18, 196–1.
- Botstein, D., Sherlock, G., Cantor, M., Troyanskaya, O., Brown, P., Tibshirani, R., Altman, R.B., Hastie, T., 2001. Missing value estimation methods for DNA microarrays . *Bioinformatics* 17, 520–525. doi:[10.1093/bioinformatics/17.6.520](https://doi.org/10.1093/bioinformatics/17.6.520).
- Bronstein, M.M., Bruna, J., LeCun, Y., Szlam, A., Vandergheynst, P., 2017. Geometric deep learning: going beyond euclidean data. *IEEE Signal Processing Magazine* 34, 18–42.
- Bruna, J., Zaremba, W., Szlam, A., LeCun, Y., 2013. Spectral networks and locally connected networks on graphs. arXiv preprint arXiv:1312.6203 .
- Che, Z., Purushotham, S., Cho, K., Sontag, D., Liu, Y., 2018. Recurrent neural networks for multivariate time series with missing values. *Scientific Reports* 8, 6085.
- Chen, H., Engkvist, O., Wang, Y., Olivecrona, M., Blaschke, T., 2018. The rise of deep learning in drug discovery. *Drug Discovery Today* 23, 1241–1250.
- Defferrard, M., Bresson, X., Vandergheynst, P., 2016. Convolutional neural



- networks on graphs with fast localized spectral filtering, in: *Advances in Neural Information Processing Systems*, pp. 3844–3852.
- Dua, D., Graff, C., 2017. UCI machine learning repository. URL: <http://archive.ics.uci.edu/ml>.
- Gallicchio, C., Micheli, A., 2013. Tree echo state networks. *Neurocomputing* 101, 319–337.
- Gama, F., Marques, A.G., Leus, G., Ribeiro, A., 2019. Convolutional neural network architectures for signals supported on graphs. *IEEE Transactions on Signal Processing* 67, 1034–1049.
- Gilmer, J., Schoenholz, S.S., Riley, P.F., Vinyals, O., Dahl, G.E., 2017. Neural message passing for quantum chemistry, in: *Proc. 34th International Conference on Machine Learning (ICML)*, JMLR. org. pp. 1263–1272.
- Gondara, L., Wang, K., 2018. Multiple imputation using deep denoising autoencoders, in: *Proc. 22nd Pacific-Asia Conference on Knowledge Discovery and Data Mining (PAKDD)*, pp. 1–12.
- Goodfellow, I., Bengio, Y., Courville, A., 2016. *Deep learning*. MIT Press.
- Goodfellow, I., Pouget-Abadie, J., Mirza, M., Xu, B., Warde-Farley, D., Ozair, S., Courville, A., Bengio, Y., 2014. Generative adversarial nets, in: *Advances in Neural Information Processing Systems*, pp. 2672–2680.
- Gori, M., Monfardini, G., Scarselli, F., 2005. A new model for learning in graph domains, in: *Proc. 2005 IEEE International Joint Conference on Neural Networks (IJCNN)*, IEEE. pp. 729–734.

- Gulrajani, I., Ahmed, F., Arjovsky, M., Dumoulin, V., Courville, A.C., 2017. Improved training of wasserstein gans, in: *Advances in Neural Information Processing Systems*, pp. 5767–5777.
- He, K., Zhang, X., Ren, S., Sun, J., 2016. Deep residual learning for image recognition, in: *Proceedings 2016 IEEE Conference on Computer Vision and Pattern Recognition (ICCVPR)*, pp. 770–778.
- Ker, J., Wang, L., Rao, J., Lim, T., 2018. Deep learning applications in medical image analysis. *IEEE Access* 6, 9375–9389.
- Kingma, D.P., Ba, J., 2014. Adam: A method for stochastic optimization, in: *Proc. 3rd International Conference for Learning Representations (ICLR)*.
- Kipf, T.N., Welling, M., 2017. Semi-supervised classification with graph convolutional networks, in: *Proc. 2017 International Conference on Learning Representations (ICLR)*.
- Lakshminarayan, K., Harp, S.A., Goldman, R.P., Samad, T., et al., 1996. Imputation of missing data using machine learning techniques., in: *Proc. KDD-96*, pp. 140–145.
- Li, Y., Tarlow, D., Brockschmidt, M., Zemel, R., 2015. Gated graph sequence neural networks, in: *Proc. 2016 International Conference on Learning Representations (ICLR)*, pp. 1–20.
- Little, R.J.A., Rubin, D.B., 1986. *Statistical Analysis with Missing Data*. John Wiley & Sons, Inc., New York, NY, USA.

- Nazabal, A., Olmos, P.M., Ghahramani, Z., Valera, I., 2018. Handling incomplete heterogeneous data using vaes. arXiv preprint arXiv:1807.03653 .
- Pennington, J., Socher, R., Manning, C., 2014. Glove: Global vectors for word representation, in: Proc. 2014 Conference on Empirical Methods in Natural Language Processing (EMNLP), pp. 1532–1543.
- Sandryhaila, A., Moura, J.M., 2013. Discrete signal processing on graphs. IEEE Transactions on Signal Processing 61, 1644–1656.
- Sardellitti, S., Barbarossa, S., Di Lorenzo, P., 2017. On the graph fourier transform for directed graphs. IEEE Journal of Selected Topics in Signal Processing 11, 796–811.
- Scarselli, F., Gori, M., Tsoi, A.C., Hagenbuchner, M., Monfardini, G., 2009. The graph neural network model. IEEE Transactions on Neural Networks 20, 61–80.
- Schlichtkrull, M., Kipf, T.N., Bloem, P., Van Den Berg, R., Titov, I., Welling, M., 2018. Modeling relational data with graph convolutional networks, in: European Semantic Web Conference, Springer. pp. 593–607.
- Śmieja, M., Struski, Ł., Tabor, J., Zieliński, B., Spurek, P., 2018. Processing of missing data by neural networks, in: Advances in Neural Information Processing Systems, pp. 2724–2734.
- Stekhoven, D.J., Buehlmann, P., 2012. Missforest - non-parametric missing value imputation for mixed-type data. Bioinformatics 28, 112–118.

- Van Buuren, S., 2018. Flexible imputation of missing data. Chapman and Hall/CRC.
- van Buuren, S., Groothuis-Oudshoorn, K., 2011. mice: Multivariate imputation by chained equations in r. *Journal of Statistical Software* 45, 1–67.
- Veličković, P., Cucurull, G., Casanova, A., Romero, A., Lio, P., Bengio, Y., 2018. Graph attention networks, in: Proc. 2018 International Conference on Learning Representations (ICLR).
- Villani, C., 2008. Optimal transport – Old and new. Springer Science & Business Media.
- Vincent, P., Larochelle, H., Bengio, Y., Manzagol, P.A., 2008. Extracting and composing robust features with denoising autoencoders, in: Proc. 25th International Conference on Machine Learning (ICML), ACM, New York, NY, USA. pp. 1096–1103.
- Wang, X., Girshick, R., Gupta, A., He, K., 2018. Non-local neural networks, in: Proc. IEEE Conference on Computer Vision and Pattern Recognition (ICCVPR), pp. 7794–7803.
- Wang, X., Li, A., Jiang, Z., Feng, H., 2006. Missing value estimation for dna microarray gene expression data by support vector regression imputation and orthogonal coding scheme. *BMC Bioinformatics* 7, 32.
- White, I.R., Royston, P., Wood, A.M., 2011. Multiple imputation using chained equations: issues and guidance for practice. *Statistics in Medicine* 30, 377–399.

- Ying, R., He, R., Chen, K., Eksombatchai, P., Hamilton, W.L., Leskovec, J., 2018. Graph convolutional neural networks for web-scale recommender systems, in: Proc. 24th ACM SIGKDD International Conference on Knowledge Discovery & Data Mining, ACM. pp. 974–983.
- Yoon, J., Jordon, J., van der Schaar, M., 2018. Gain: Missing data imputation using generative adversarial nets, in: Proc. 35th International Conference of Machine Learning (ICML), pp. 1–10.
- Zhang, H., Wang, S., Xu, X., Chow, T.W., Wu, Q.J., 2018. Tree2vector: learning a vectorial representation for tree-structured data. *IEEE Transactions on Neural Networks and Learning Systems* 28, 5304–5318.